Anomalous Exciton Diffusion in the Conjugated Polymer MEH−PPV Measured Using a Three-Pulse Pump−Dump−Probe Anisotropy Experiment

Kevin M. Gaab and Christopher J. Bardeen*

Department of Chemistry, University of Illinois, 600 South Mathews Avenue, Urbana, Illinois 61801

Received: August 6, 2004; In Final Form: September 23, 2004

A femtosecond pump−dump−probe anisotropy experiment is used to study the time-dependent motion of singlet excitons in the conjugated polymer poly[2-methoxy-5-((2-ethylhexyl)oxy)-1,4-phenylenevinylene] (MEH−PPV). The pump pulse prepares an unpolarized population of excitons at time $t = 0$, which is then depleted by a linearly polarized dump pulse at $t = T_{12}$. The anisotropy decay of the remaining population is then monitored as a function of the probe delay, T_{23}. At both room temperature and 4 K, the T_{23} anisotropy decay is observed to slow as T_{12} increases. Although interpretation of our results is complicated by the possible presence of excited-state absorption at 600 nm, the wavelength of the dump and probe pulses, the T_{12} dependence is consistent with a slowing down of the diffusion of the luminescent exciton during its lifetime in the material. This experiment provides a way to directly probe anomalous diffusion of the exciton at different points during its lifetime, which is what ultimately determines the distance it can travel in the polymer.

Electronic energy transfer (EET) in conjugated organic polymers plays a central role in the diverse applications of these materials, from sensors to light-emitting diodes to solar cells.[1−3] A quantitative understanding of the factors that govern the rate and length of EET is vital for the rational design of materials with enhanced (or suppressed) energy transport properties. EET in disordered systems is usually analyzed within the framework of diffusion theory, and using this approach, one can define a diffusion coefficient D and estimate the three-dimensional diffusion length L_D of an exciton using the relation

$$L_D = \sqrt{6D\tau_{\mathrm{fl}}} \tag{1}$$

where τ_{fl} is the excited-state lifetime. Depending on the time scale and length scale of measurement, however, this picture of "normal" diffusion can break down. Energetic disorder can lead to a situation where the exciton diffuses quickly at early times but slows down at later times, for example, as it reaches a low-energy site where there are no other energetically accessible sites within the range of the transfer interaction.[4] This slowing down of the exciton motion leads to an "anomalous" or time-dependent diffusion coefficient.[5,6] Such time-dependent transport can have important practical consequences, for example, in the generation rate of free charges from singlet excitons in photovoltaic cells.[7]

Recently, we performed time- and frequency-resolved pump−probe polarization anisotropy experiments on the widely studied, amorphous conjugated polymer poly[2-methoxy-5-((2-ethylhexyl)oxy)-1,4-phenylenevinylene] (MEH−PPV).[8] Analysis of these two-pulse experiments provided information about the rate of energy transfer from an initially excited chromophore to its neighbors[9] and, assuming normal diffusion, about the overall spatial motion of the exciton. Several aspects of our data, however, suggested that the exciton motion could not be described in terms of normal diffusion. First, there was a strong dependence of the anisotropy decay time T_{pol} on excitation wavelength, indicating dispersive EET dynamics.[10] This observation could be quantitatively explained in terms of an initial EET rate that depended on where the exciton was created within an inhomogeneous distribution of chromophore energies. Second, although the anisotropy decays showed the expected $e^{-\sqrt{t}/T_{\mathrm{pol}}}$ time dependence, they always possessed small constant offsets that indicated the polarization was never completely randomized by the EET. This failure of the anisotropy to completely decay suggested that the rapid depolarization observed after photoexcitation did not proceed at the same rate over the course the exciton's lifetime. Both observations indicate that energetic disorder in MEH−PPV, as observed in single molecule experiments,[11,12] may play an important role in EET.

Though our earlier work provided evidence in MEH−PPV, it could not address whether these different energetic environments were coupled, which would lead to anomalous exciton diffusion at longer times. Two-pulse pump−probe experiments, and, in fact, any $\chi^{(3)}$ experiment designed to probe rotational diffusion, can only measure the loss of anisotropy during a single time interval immediately after photoexcitation. If the bath is stationary, meaning that the statistical mechanical nature of the environment does not evolve during the excited-state lifetime of the probe, then it does not matter when one probes the diffusion—immediately after absorption of a photon, or much later—the measured diffusion rate will always be the same. But it is straightforward to picture situations where the stationary condition breaks down. One example is a chromophore in solution whose charge distribution in the excited state undergoes a large change relative to the ground state. If the local solvent must rearrange to accommodate the new charge distribution, then the local friction experienced by the solute (and thus its rotational diffusion rate) can change with time as well. In a similar manner, as an exciton diffuses through a disordered medium, its immediate surroundings change and thus the probability that it continues to diffuse changes as well. Again, the bath appears to be nonstationary, but now because the

* Corresponding author. Phone: 217-265-5017. Fax: 217-244-3186. E-mail: bardeen@uiuc.edu.

10.1021/jp0464472 CCC: $27.50
Published on Web 11/13/2004

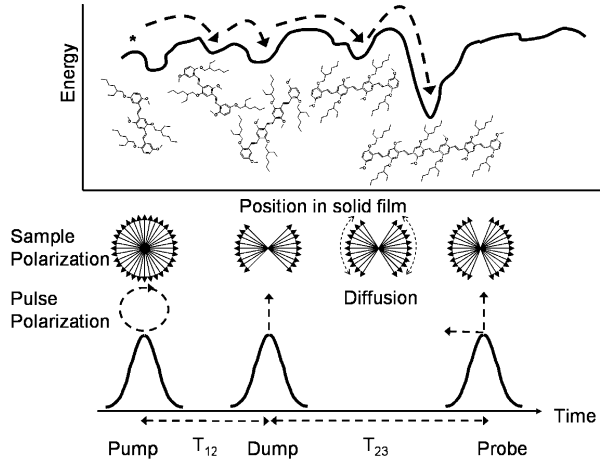

Figure 1. Diagramatic representation of the experimental three-pulse experiment. The circularly polarized pump pulse (400 nm) creates an isotropic excited-state distribution in the sample. This is followed by a linearly polarized dump pulse (600 nm) at time T_{12}, which creates a polarization "hole" in the excited state. This hole is filled in via exciton diffusion in the sample and is probed at time T_{23} by the probe pulse (600 nm).

excitation travels between different chromophores in different environments. Two-pulse experiments at multiple wavelengths, like those reported in ref 8, can tell us about the existence of these different environments, but they cannot provide the information we really need to understand transport, namely how do excitons move between these environments, and how quickly does the rapid motion observed immediately after photoexcitation get quenched as the exciton moves to progressively lower energy sites. A loose analogy may be drawn between our study of rotational dynamics, which probe physical motion through real space, and the study of spectral line shapes, which reflect the motion of a quantum state through energy space. Spectral broadening may be studied in the time domain using the free induction decay, a $\chi^{(1)}$ process, but multiple pulse $\chi^{(3)}$ spectroscopies such as the photon echo are required if one wants to quantify longer time phenomena like spectral diffusion. Because energy level shifts affect the electronic polarization terms in the density matrix description of optical spectroscopy,[13] each field interaction can manipulate this polarization and $\chi^{(3)}$ spectroscopies are sufficient to provide multiple experimental time delays. To quantify the longer time rotational diffusion also requires multiple pulse methods, but now intensity (field squared) interactions must be used to manipulate populations rather than polarizations.

We have recently developed a three-pulse pump−dump−probe anisotropy experiment to directly observe such longer time dynamics in EET.[14] Technically a $\chi^{(5)}$ process, it is related in spirit to recent experiments designed to probe solvation.[15,16] The experiment is outlined in Figure 1 in the context of EET in a disordered system. In this experiment, a circularly polarized pump pulse creates an isotropic excited-state population at $t = 0$. This population undergoes various relaxation processes, but there is no observable polarization in the sample until T_{12}. At that time, a second (dump) pulse, linearly polarized and shifted in wavelength to overlap the excited-state emission, depletes the excited-state population and leaves a polarized hole. The polarization anisotropy of the depleted excited-state decays as the remaining excited-state molecules transfer energy to their randomly oriented neighbors. The decay of the dump-induced anisotropy is then measured by a third (probe) pulse whose delay T_{23} is scanned. The dump−probe sequence is the equivalent of a two-pulse anisotropy experiment on the nonstationary excited-state population, and the analysis of the T_{23} anisotropy decay is identical to that in the standard two-pulse case. Although the signal is lower than in $\chi^{(3)}$ experiments, one can acquire multiple T_{23} anisotropy decays which depend parametrically on the pump−dump delay T_{12}.

Experiment

The samples are prepared by dissolving 5−7 mg/mL of MEH−PPV (Sigma-Aldrich, average MW ~ 51 000) in methylene chloride. The resulting solutions are stirred at room temperature for several days and then spin cast onto 1 mm thick glass substrates at 600 rpm for 600 s to yield films with a peak optical density of between 0.5 and 1.0. The thin films are immediately loaded into a Janis ST-100 continuous-flow cryostat and placed under vacuum to prevent photooxidative damage. Steady-state absorption and fluorescence spectra were taken using an Ocean Optics S-2000 UV−vis spectrometer and 400 nm excitation. The pump−dump−probe experiments are performed using a 40 kHz regeneratively amplified Ti:sapphire laser system. Its frequency-doubled output provides the 400 nm pump pulse and also pumps a noncollinear optical parametric amplifier, whose output is tuned to 600 nm, near the peak of the MEH−PPV fluorescence, to generate the dump and probe pulses. The visible pulse, with a bandwidth of ~16−20 nm, is passed through a prism compressor and the intensity autocorrelation widths of 40−50 fs are obtained by second harmonic generation in a 0.1 mm BBO crystal. The cross-correlation of the 400 nm/600 nm pulses is measured by detecting fluorescence generated by the two-photon absorption of *p*-terphenyl in a PMMA film, yielding widths 110−135 fs. All the beams are passed through calcite polarizers to purify their polarizations immediately before the experiment. The pump pulses are circularly polarized using a $^1/_4$-wave plate and the polarization of the probe pulse is oriented 45° relative to that of the dump. After the sample, the probe beam is directed into a polarizer set at 90°, which splits the beam into its parallel and perpendicular components, which are detected separately. In this detection scheme, induced birefringence effects due to different polarizabilities in the ground and excited states[17,18] are eliminated from the signal, which only reflects the linear dichroism of the sample. The pump and dump beams are mechanically chopped and the differential transmittance of the probe beam is detected at the sum frequency. The three laser beams are focused to a spot with a diameter of ~100 μm, and the probe fluence is on the order of 0.1 μJ/cm^2. The 400 nm excitation fluence at the sample is ~5 μJ/cm^2, whereas the 600 nm dump fluence is ~45 μJ/cm^2, resulting in a maximum differential transmittance $\Delta T/T$ of ~10^{-4} at 600 nm. Varying either the pump or dump powers by a factor of 2 did not change the observed anisotropy dynamics, and previous degenerate pump−probe experiments suggest any intensity-dependent dynamics are isotropic and do not influence the anisotropy decays.[8]

Results and Discussion

Figure 2 depicts the absorption and emission spectra for MEH−PPV thin films at both room temperature and 4 K, as well as the power spectra of the 400 nm (pump) and 600 nm (dump/probe) pulses. As the temperature is lowered, both the absorption and emission shift to longer wavelengths and sharpen. This shift is larger for the emission, and this leads to a corresponding decrease in their spectral overlap. In both cases, however, the 600 nm dump/probe sequence has good overlap with the emission.

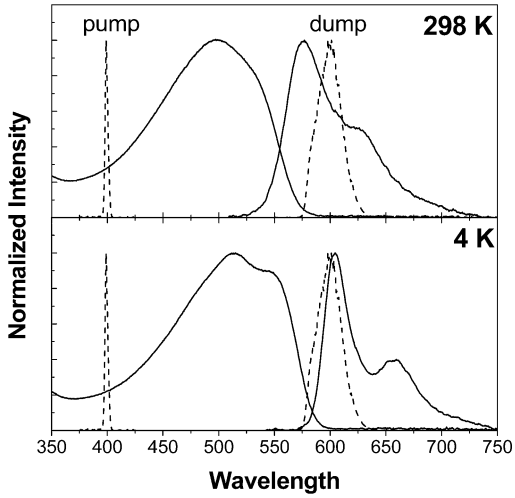

Figure 2. Steady-state absorption and emission spectra for MEH−PPV thin film (solid) and spectral profile for the 400 nm pump and 600 nm dump/probe pulses (dashed).

The normalized three-pulse anisotropy decays at T_{12} delays of 1, 21, and 42 ps are shown in Figure 3. In all cases, the initial T_{23} anisotropies were reproducibly ∼0.33. We note that the 400 nm excitation fluences used in this experiment result in an intensity-dependent decay of the stimulated emission signal, most likely due to exciton−exciton annihilation.[19−21] This fluence was necessary to achieve acceptable signal-to-noise ratios, but the more rapid population decay caused the pump−dump−probe signal to decrease more rapidly than would be predicted by MEH−PPV's excited-state lifetime of ∼300 ps, which is measured using much lower fluences. Because of this more rapid decay, we were unable to obtain decays at longer T_{12} delays. Our previous results indicated that exciton−exciton annihilation is an isotropic process that proceeds independently of the EET responsible for the anisotropy decay. The anisotropy data are fit in terms of the parameters used to fit our earlier two-pulse anisotropy data,[8,22]

$$r(t) = \frac{I_{\parallel} - I_{\perp}}{I_{\parallel} + I_{\perp}} = r_0 \exp\left[-\frac{\sqrt{t}}{T_{\mathrm{pol}}}\right] + y_0 \qquad (2)$$

This expression assumes that the chromophore dipoles are randomly oriented in a plane perpendicular to the direction of the laser propagation. Although we did not characterize the in-plane orientation of the samples used in the present experiments, we have no reason to believe that they are significantly different from previously studied MEH−PPV films. There is considerable evidence from ellipsometry,[23,24] optical waveguiding,[25] reflectance,[26] and X-ray diffraction[27] that MEH−PPV chains in films made by spin coating and even drop casting lie almost entirely parallel to the substrate. Nevertheless, we have also analyzed our data using the standard expression for three-dimensional rotational diffusion and found no difference in the observed trends with T_{12}, and less than 5% difference in the extracted T_{pol} values extracted from the T_{23} decays. We fit the 298 and 4 K data at the T_{12} delays of 1, 21, and 42 ps and extract the T_{pol} values shown in Figure 4. For the fits to the normalized data, the value of y_0 was fixed at 0.1 at 298 K and 0.0 at 4 K. T_{pol} shows a strong dependence on T_{12} at both temperatures, but the dependence is most pronounced at 4 K.

Although the data in Figures 3 and 4 clearly imply a slowing in the T_{23} anisotropy decay with increasing T_{12}, indicative of anomalous subdiffusion, there are two aspects of the data that are qualitatively different from what was observed in our previous application of the pump−dump−probe technique to the rotational diffusion of Coumarin 153 (C153) in solution.[14] First, the r_0's of the T_{23} decays are consistently smaller than the theoretical maximum of 0.5, and also smaller than the values of 0.43−0.47 observed in our previous degenerate pump−probe experiments. In C153, the initial anisotropies were identical to within the experimental error for both types of experiments. Second, the two-pulse decay is clearly faster than the three-pulse decays. Figure 5 compares the normalized two-pulse 400−600 pump−probe anisotropy decays to the $T_{12} = 1$ ps and T_{23} decays at 4 and 290 K. The two-pulse data are very close to the decays obtained earlier from degenerate pump−probe experiments at short wavelengths (500 nm),[8] but the r_0 is ∼0.15 rather than 0.45. Because 400 nm is on the high-energy side of the first absorption band (see Figure 2), it accesses multiple higher lying excited states with different transition orientations,[28] which is expected to lower the r_0. More importantly, the $T_{12} =$ 1 ps three-pulse decay is always slower than the two-pulse decay, and this difference is most pronounced at 4 K. Again, this was not observed for C153, where the three-pulse decays for short T_{12} delays reproduced the two-pulse experiments. Although we examined T_{12} delays as short as ∼300 fs, these showed no significant difference from the $T_{12} \sim 1$ ps data shown in Figure 5.

The lack of agreement between the two-pulse and three-pulse anisotropy experiments in MEH−PPV is troubling, especially when compared to the simpler behavior of C153 in solution. One possible explanation for this discrepancy is the possibility that the anisotropy-inducing pulse (the pump in the two-pulse

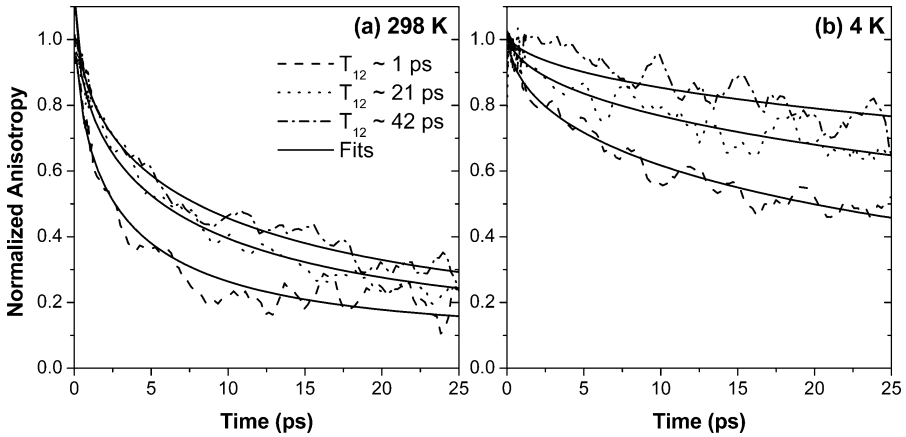

Figure 3. Normalized three-pulse anisotropy decays at 298 K (a) and 4 K (b) for T_{12} delays of ∼1 ps (dash), ∼21 ps (dot), and ∼42 ps (dot−dash), and the corresponding fits (solid).

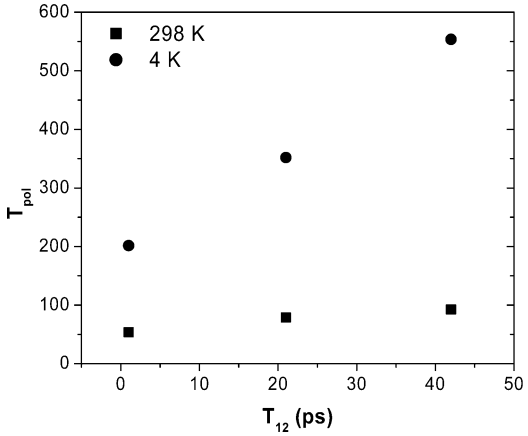

Figure 4. Plot of the fit parameter T_{pol} against the delay between the pump and dump, T_{12}, for 298 K (■) and 4 K (●).

experiment and the dump in the three-pulse experiment) interacts with different initial distributions in the two experiments. If the assumption of planar chains discussed above is correct, then circularly polarized light leads to a truly isotropic distribution of excited states in the $x-y$ plane. But if the chains lie randomly in all three dimensions, then the distribution excited by the $x-y$ circularly polarized light is not isotropic in the z-direction, and thus the two-pulse pump and three-pulse dump would interact with different initial transition dipole distributions. In the two-pulse case, the pump interacts with a spherical distribution, whereas in the three-pulse case the dump would interact with a partially relaxed doughnut-like $\sin(\theta)^2$ distribution. This was actually the case in our earlier studies of C153 rotational diffusion, but in that case there was also no observable difference between the two- and three-pulse results.[14] In fact, although it is beyond the scope of this paper, it can be shown that the details of the initial distribution along the z-axis are of little importance in determining the relaxation observed by light polarized along the x- and y-axes.

A more likely explanation for the divergence of the two- and three-pulse data lies in the complex photophysics of MEH−PPV. Previous workers have shown the existence of an excited-state absorption (ESA) contribution at 600 nm,[29,30] most likely due to an excimer type state, which has been invoked to explain differences between time-resolved luminescence and transient absorption data.[21] The relative intensity of this ESA depends on sample preparation,[31,32] but it is present even in carefully prepared samples. If excitation at 400 nm creates a variety of species, some of which preferentially absorb at 600 nm and some of which emit,[30,31] we have the situation outlined in Figure 6. In the two-pulse 400−600 experiment, the 600 nm probe pulse actually measures different transitions, both emission from the luminescent-state B to the ground-state S_0, and from state A to higher excited states. Similar to pumping at 400 nm, dumping at 600 nm would also lead to transitions between multiple states with different transition dipole orientations. In both cases, because the absorption/emission event is not purely to a single state, the initial anisotropy will be lower than 0.5, because the two nonparallel transitions will act to depolarize the total signal at that wavelength. Near the peak of the MEH−PPV absorption, where we performed our previous degenerate pump−probe experiments, the absorption should be dominated by a single excited state, which would explain the higher r_0's seen in those experiments. The discrepancy between the two- and three-pulse anisotropy dynamics shown in Figure 5 could also result from the situation in Figure 6. When the 600 nm dump pulse creates the anisotropy, it will populate both the higher lying excited states and the ground state through both ESA and stimulated emission. Species A undergoes absorption at 600 nm, which contributes to the decreased initial anisotropy, but according to Kasha's rule, it should relax quickly to their original state. If this relaxation occurs within a few hundred femtoseconds, it will not contribute significantly to the dynamics observed during the picosecond T_{23} period. The dynamics will be dominated by the much longer lived depletion of the emitting state, rather than the transient population in the higher lying excited states. If this is the case, the pump−dump−probe experiment is most sensitive to the dynamics of the luminescent singlet excitons, rather than polarons or excimers, a possible advantage of the technique. In any case, the presence of multiple spectroscopic species in MEH−PPV provides a reasonable explanation of the divergence of the two- and three-pulse anisotropy data. An obvious improvement of the technique would be to use a pump−dump−upconvert experiment, where fluorescence upconversion is used to monitor the exciton without the complications from ESA that are present in the transient absorption probing method used here.

Though the possible presence of an ESA component at 600 nm complicates the analysis, the T_{12} dependence of the T_{23} decay cannot be ascribed solely to ESA dynamics. First, the r_0 values of the three-pulse experiments do not change with T_{12}, as would be expected if the ESA contribution was changing significantly on the experimental time scale. Second, the systematic slowing down of the anisotropy decay with T_{12}, which is directly related to the spatial motion of the exciton, is exactly what is expected

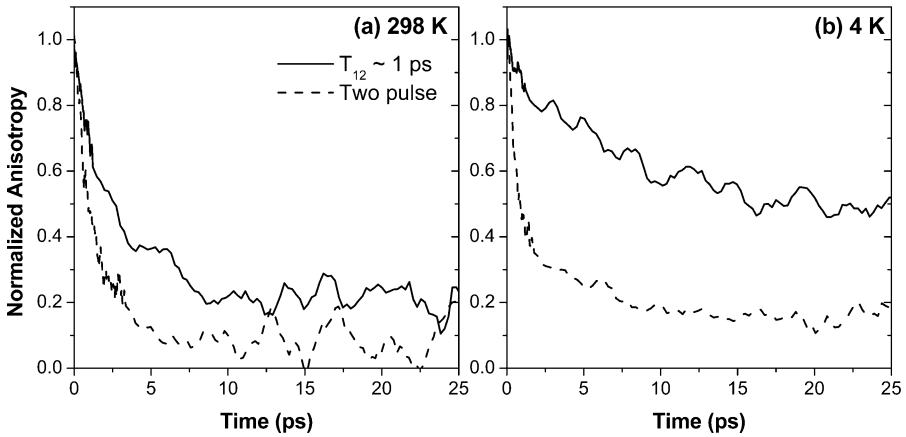

Figure 5. Normalized three-pulse anisotropy decays at 298 K (a) and 4 K (b) for T_{12} delay of ~1 ps (solid), compared with the normalized two-pulse 400−600 pump−probe anisotropy decays.

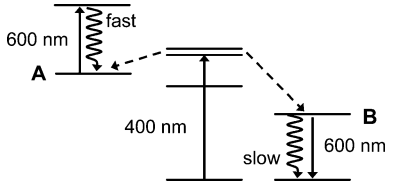

Figure 6. Proposed scheme to explain the initial anisotropy different dynamics seen in the two- and three-pulse anisotropy decays. In the two-pulse experiment, the decay of the anisotropy induced at 400 nm reflects the dynamics of both species A and B. In the three-pulse experiment, the 600 nm dump pulse interacts with A and B as well, but only the depleted population in the emissive state B survives long enough to affect the picosecond T_{23} decay.

from anomalous diffusion. In fact, earlier theories of exciton motion predict a transition between an anomalous regime and a normal regime, although a complete analytical solution to the problem remains to be found.[33−37] Third, the strong temperature dependence of the data seen in Figure 4 is further evidence that this picosecond slowing down of the anisotropy decay is not merely due to intramolecular ESA shifting. Bassler and coworkers have explored the effect of energetic disorder on exciton transport in a variety of systems under various types of transfer mechanisms, mainly using numerical simulations and fluorescence shifting experiments.[4,38,39] The large temperature effect observed in our data is qualitatively similar to what is expected on the basis of their theory.[40] We note that lowering the temperature has very little effect on the 400−600 two-pulse data, which provides further evidence that this decay is sensitive to processes other than luminescent exciton diffusion. Equation 2 should be viewed as a convenient way to parametrize our data, because many of the assumptions underlying its derivation (no energetic disorder, point-dipole Forster transfer) probably do not hold for MEH−PPV. Nevertheless, it is interesting to explore the implications of the T_{12} dependence of T_{pol} on the expected diffusion coefficient D, using the relation[22]

$$D = \left(\frac{4}{3}\pi\rho\right)^{-2/3} \frac{A}{(\lambda^{-1/2}\gamma\Gamma(1/2))^2} \frac{1}{T_{\mathrm{pol}}{}^2} \qquad (3)$$

where ρ is the number density of chromophores, A is a constant ranging between 0.30 and 0.50, $\Gamma(x)$ is the gamma function, γ is a factor that takes orientational disorder into account, and λ is either 1 or 2 depending on whether back-transfer is allowed in the system. From Figure 4 and eq 3, we estimate that the exciton's diffusion rate decreases by ∼67% within the first 50 ps of its lifetime at 298 K and ∼87% at 4 K, with corresponding reductions in its spatial displacement. Clearly, this effect can significantly impact the material's energy transport properties.

In summary, this work shows how the three-pulse pump−dump−probe anisotropy experiment can be applied to EET dynamics in a dense chromophoric system. The photophysics of MEH−PPV, with multiple states accessed by the exciting pulses and the possible role of ESA, makes interpretation of our data in terms of a two-state system, as in the case of C153, impossible. Even taking these complications into account, however, the data in this paper confirm the existence of an anomalous, time-dependent slowing-down of the exciton diffusion in this conjugated polymer. These direct measurements provide a way to begin to quantify the time-dependent diffusion whose existence could only be inferred from two-pulse experiments. Our results are consistent with previous theoretical predictions based on considerations of exciton motion in disordered systems, as well as our previous two-pulse results. As in biological light-harvesting complexes,[41,42] other nonlinear optical experiments such as the three-pulse photon echo may help clarify the extent and detailed nature of energetic disorder in MEH−PPV.[43] Another approach is to study concentrated solutions of monomeric chromophores whose structures are well-known and whose spectroscopy can be characterized. By avoiding questions of sample heterogeneity and multiple species, such experiments should alleviate the difficulties encountered in our interpretation of the MEH−PPV data. We are currently pursuing this approach using perylene derivatives dissolved in amorphous polymers.

Acknowledgment. This work is supported by NSF grant CHE-0415981. C.J.B. is a Sloan Research Fellow, and K.M.G. is an Ullyot Fellow at UIUC.

References and Notes

(1) McQuade, D. T.; Pullen, A. E.; Swager, T. M. *Chem. Rev.* **2000**, *100*, 2537−2574.
(2) Brabec, C. J.; Sariciftci, N. S.; Hummelen, J. C. *Adv. Funct. Mater.* **2001**, *11*, 15−26.
(3) Friend, R. H.; Gymer, R. W.; Holmes, A. B.; Burroughes, J. H.; Marks, R. N.; Taliani, C.; Bradley, D. D. C.; Santos, D. A. D.; Bredas, J. L.; Logdlund, M.; Salaneck, W. R. *Nature* **1999**, *397*, 121−128.
(4) Movaghar, B.; Grunewald, M.; Ries, B.; Bassler, H.; Wurtz, D. *Phys. Rev. B* **1986**, *33*, 5545−5554.
(5) Pfister, G.; Scher, H. *Adv. Phys.* **1978**, *27*, 747−798.
(6) Metzler, R.; Klafter, J. *Phys. Rep.* **2000**, *339*, 1−77.
(7) Arkhipov, V. I.; Emelianova, E. V.; Bassler, H. *Chem. Phys. Lett.* **2004**, *383*, 166−170.
(8) Gaab, K. M.; Bardeen, C. J. *J. Phys. Chem. B* **2004**, *108*, 4619−4626.
(9) Gochanour, C. R.; Fayer, M. D. *J. Phys. Chem.* **1981**, *85*, 1989−1994.
(10) Stein, A. D.; Peterson, K. A.; Fayer, M. D. *J. Chem. Phys.* **1990**, *92*, 5622−5635.
(11) Yu, J.; Hu, D.; Barbara, P. F. *Science* **2000**, *289*, 1327−1330.
(12) Yu, Z.; Barbara, P. F. *J. Phys. Chem. B* **2004**, *108*, 11321−11326.
(13) Mukamel, S. *Principles of Nonlinear Optical Spectroscopy*; Oxford: New York, 1995.
(14) Gaab, K. M.; Bardeen, C. J. *Phys. Rev. Lett.* **2004**, *93*, 056001.
(15) Underwood, D.; Blank, D. A. *J. Phys. Chem. A* **2003**, *107*, 956−961.
(16) Park, S.; Flanders, B. N.; Shang, X.; Westervelt, R. A.; Kim, J.; Scherer, N. F. *J. Chem. Phys.* **2003**, *118*, 3917−3920.
(17) Waldeck, D.; Cross, A. J.; McDonald, D. B.; Fleming, G. R. *J. Chem. Phys.* **1981**, *74*, 3381−3387.
(18) Beddard, G. S.; Westby, M. J. *Chem. Phys.* **1981**, *57*, 121−127.
(19) Maniloff, E. S.; Klimov, V. I.; Mcbranch, D. W. *Phys. Rev. B* **1997**, *56*, 1876−1881.
(20) Moses, D.; Dogariu, A.; Heeger, A. J. *Chem. Phys. Lett.* **2000**, *316*, 356−360.
(21) Martini, I. B.; Smith, A. D.; Schwartz, B. J. *Phys. Rev. B* **2004**, *69*, 035204.
(22) Baumann, J.; Fayer, M. D. *J. Chem. Phys.* **1986**, *85*, 4087−4107.
(23) Tammer, M.; Monkman, A. P. *Adv. Mater.* **2002**, *14*, 210−212.
(24) Ramsdale, C. M.; Greenham, N. C. *Adv. Mater.* **2002**, *14*, 212−215.
(25) Boudrioua, A.; Hobson, P. A.; Matterson, B.; Samuel, I. D. W.; Barnes, W. L. *Synth. Met.* **2000**, *111−112*, 545−547.
(26) McBranch, D.; Campbell, I. H.; Smith, D. L.; Ferraris, J. P. *Appl. Phys. Lett.* **1995**, *66*, 1175−1177.
(27) Yang, C. Y.; Hide, F.; Diaz-Garcia, M. A.; Heeger, A. J.; Cao, Y. *Polymer* **1998**, *39*, 2299−2304.
(28) Martin, S. J.; Bradley, D. D. C.; Lane, P. A.; Mellor, H.; Burn, P. L. *Phys. Rev. B* **1999**, *59*, 15133−15142.
(29) Hsu, J. W. P.; Yan, M.; Jedju, T. M.; Rothberg, L. J.; Hsieh, B. R. *Phys. Rev. B* **1994**, *49*, 712−715.
(30) Yan, M.; Rothberg, L. J.; Kwock, E. W.; Miller, T. M. *Phys. Rev. Lett.* **1995**, *75*, 1992−1995.
(31) Nguyen, T.; Doan, V.; Schwartz, B. J. *J. Chem. Phys.* **1999**, *110*, 4068−4078.
(32) Nguyen, T.; Wu, J.; Doan, V.; Schwartz, B. J.; Tolbert, S. H. *Science* **2000**, *288*, 652−656.
(33) Gochanour, C. R.; Andersen, H. C.; Fayer, M. D. *J. Chem. Phys.* **1979**, *70*, 4254−4271.

(34) Godzik, K.; Jortner, J. *J. Chem. Phys.* **1980**, *72*, 4471−4486.
(35) Haan, S. W.; Zwanzig, R. *J. Chem. Phys.* **1978**, *68*, 1879−1883.
(36) Klafter, J.; Silbey, R. *J. Chem. Phys.* **1980**, *72*, 843−852.
(37) Fedorenko, S. G.; Burshtein, A. I. *Chem. Phys.* **1985**, *98*, 341−349.
(38) Bassler, H.; Schweitzer, B. *Acc. Chem. Res.* **1999**, *32*, 173−182.
(39) Meskers, S. C. J.; Hubner, J.; Oestreich, M.; Bassler, H. *J. Phys. Chem. B* **2001**, *105*, 9139−9149.
(40) Schonherr, G.; Eiermann, R.; Bassler, H.; Silver, M. *Chem. Phys.* **1980**, *52*, 287−298.
(41) Agarwal, R.; Rizvi, A. H.; Prall, B. S.; Olsen, J. D.; Hunter, C. N.; Fleming, G. R. *J. Phys. Chem. A* **2002**, *106*, 7573−7578.
(42) Book, L. D.; Ostafin, A. E.; Ponomarenko, N.; Norris, J. R.; Scherer, N. F. *J. Phys. Chem. B* **2000**, *104*, 8295−8307.
(43) Scholes, G. D.; Larsen, D. S.; Fleming, G. R.; Rumbles, G.; Burn, P. L. *Phys. Rev. B* **2000**, *61*, 13670−13678.